HYDRODYNAMICS OF TRANSVERSE FLOW PAST BANKS OF TUBES

S. V. Alekseenko, S. Yu. Belov,
D. M. Markovich, and S. I. Shtork

UDC 536.24

Profiles of flow separation zones, the velocity field, and turbulent pulsations are investigated experimentally for transverse flow past staggered banks of tubes. Experimental data is compared with results of calculations.

In the design and analysis of the operation of steam boilers on low-quality brown coal, much attention is paid to processes of contamination and abrasive deterioration (erosion) of heat exchangers located in convective gas flues of the boiler, which usually consist of transverse flow past the banks of tubes. In order to evaluate the intensity of contamination or erosion it is necessary to calculate the motion of ash particles, which is dictated by the aerodynamics of the flow. Flow past a bank of tubes is followed by the formation of separation zones, turbulence, and nonstationary interaction of wakes [1]. Purely theoretical study of such complicated aerodynamics seemed to be impossible [2]; that is why attempts are made to apply approximation methods with the use of empirical data. One of those methods, comparatively easily realized, is based on datda on configuration of the separation zone behind the cylinder in the theory of an ideal liquid [3]. In this case the separation zone is modeled by a set of dipoles.

A host of studies are devoted to the investigation of hydrodynamics and heat exchange in the flow past the bank of tubes, results of which are reflected fairly completely in [1, 4]. However, there is no generalization of aerodynamic data for different banks; information on the configuration of separation zones, velocity profiles, and turbulent pulsations in the intertube space is practically absent. Therefore, the problem of the experimental study of the flow past a bank of tubes given geometry was formulated under isothermal conditions and correlation of the results obtained with the approximate theoretical models.

Two main types of banks of smooth tubes are used in tube heat exchangers: staggered and unstaggered. In the unstaggered banks the tubes are located in the nodes of a rectangular network. The defining geometric parameters of the bank are the relative transverse step $\sigma_1 = s_1/d$ and relative longitudinal step $\sigma_2 = s_2/d$ (see inset in Fig. 3). The flow regime is usually characterized by the Reynolds number $Re = U_\infty d/\nu$ (later on, we assume that the direction of flow is vertical). In the case of turbulent drag, one more parameter is added, the degree of turbulence.

In spite of strong turbulization of the flow in the depth of the bank, in the frontal part of tubes, the laminar boundary layer can be formed as before due to large negative pressure gradient. To this end, the following flow regimes are distinguished: predominantly laminar $Re < 10^3$; mixed $10^3 < Re < 1.5\cdot10^5$; predominantly turbulent $Re > 1.5\cdot10^5$. For convective heat exchangers, the typical value of $Re \sim 5\cdot10^3$ in the gas conduits of the heater, and, as is seen, the flow falls into the category of a mixed regime. It is precisely such regimes (more exactly, the range of the Reynolds numbers $Re = 10^3$–$5\cdot10^4$) that were investigated in the given work.

On the basis of the data in the literature we can draw the following conclusions about changing regularities of the flow when passing from a single cylinder to a bank. The turbulence of the drag affects only the first one-three rows. And since the rows of cylinders themselves play the role of the turbulent grids, the regime completely defined for the given geometry of the bank is attained in the depth of the bank. In a subcritical regime, the point of separation of the laminar boundary layer is moved down the flow due to a large negative pressure gradient in the bank as compared with the case of a single cylinder. But a

Krasnoyarsk State University. Translated from Inzhenerno-Fizicheskii Zhurnal, Vol. 58, No. 1, pp. 5-11, January, 1990. Original article submitted July 19, 1988.

0022-0841/90/5801-0001$12.50 © 1990 Plenum Publishing Corporation

TABLE 1. Characteristics of Investigated Banks of Tubes

No. of version	d, mm	Type of bank	σ_1	σ_2	Number of horizontal rows	Number of vertical rows
1	22	Single cylinder	—	—	—	—
2	22	Single row	2,45	—	1	—
3	13	Staggered bank	4,15	1	6	7
4	13	»	4,15	3	5	6
5	22	»	2,45	1,8	5	7
6	22	»	2,45	3	5	7

critical regime sets in earlier due to turbulization of the flow in the depth of the bank. The energy spectrum of the velocity pulsations in the first row has an explicitly expressed maximum corresponding to the frequency of separation of vortices. In the deep rows of the bank, large-scale vortices dissipate and the spectrum becomes uniform [1]. The geometric parameters σ_1 and σ_2 have a great effect on the picture of the flow.

In this work we investigated flow past a single cylinder, a row of cylinders, and four versions of banks, important for practical uses, with $\sigma_1 \times \sigma_2 = 4.15 \times 1$; 4.15×3; 2.45×1.8; 2.45×3.

The experiments were performed on a hydrodynamic bench consisting of a reservoir with a capacity of 200 liters, a centrifugal pump with an output of 8 liter/sec, a work site, connecting polyethylene tubes, and other elements. The work site was a rectangular organic glass channel with a cross-section of 162×86 mm and 510 mm in height, in which the bank of tubes was placed. The liquid was fed through a lower central opening with a diameter of 54 mm. In order to level off the flow, three grids were installed in front of the bank, the parameters of the grids and the distances between them were chosen according to [5] and were adjusted to be optimal experimentally.

The bank of tubes was modeled by a set of polished cylinders made of organic glass, which were 78 mm in length and 13 or 22 mm in diameter and were fixed on two plates (tube boards). Halves of the cylinders were mounted on the bench. Characteristics of the investigated versions of the bank are given in Table 1.

In the course of the experiment, visual investigation of the flow, measurements of the configuration of the separation zone, velocity profile, and the level of turbulent pulsations were conducted. The flow was visualized with the help of small bubbles of air illuminated laterally by a light "knife." The shape of the separation zone was determined as follows. The boundaries of the separation zone were projected onto the same drawing from 4-8 photographs taken at different moments of time. Then the graphical averaging of boundaries was done for both incident and reflected images (in order to achieve symmetrization of the profile). We only considered the part of the separation zone where vibrations of the boundary with respect to the average position did not exceed 10-15% of the width of the separation zone in the given cross-section. As a result, the boundaries of the separation zone near the surface of the cylinder were obtained averaged over time. For weakly blocked banks the averaging of the boundaries of the far part of the separation zone, where the large vortices become detached, apparently did not have a special physical sense. When the picture of flow was automodeled with respect to the Reynolds numbers or the location of the cylinder in the bank, the averaging was also done over the Reynolds numbers and different cylinders. The detailed study of the separation point did not constitute the goal of the experiment; therefore, the boundary of the separation zone was not continued to the surface of the cylinder in the figures.

Local velocities of the flow were measured with the help of the electrodiffusion method [6]. We used a velocity sensor of the type "frontal point" with outer diameter approximately equal to 70 μm. An equimolar solution of potassium ferricyanide and potassium ferrocyanide (concentration 0.005 N) in distilled water with a background admixture of sodium carbonate (Na_2CO_3) in the quantity of 0.1-0.2 M served as a working liquid. The sensors were calibrated directly on the working site or based on the readings of the standard differential Pitot tube, or with the help of an auxiliary submerged nozzle with a rectangular velocity profile on its cut-off. Since the sensor readings were fairly stable, the error in measuring the average

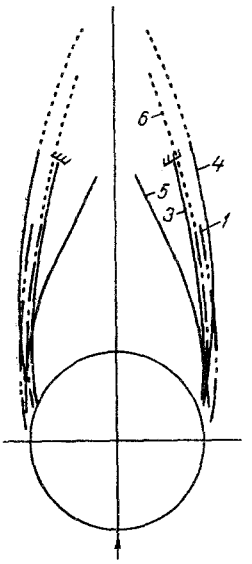

Fig. 1 Generalized profiles of the separation zones: the numbers of curves correspond to the number of the version of the bank in Table 1.

velocity was determined by the calibration and constituted 2-5%. The signal was processed on a computer.

Configuration of the Separation Zone. The main factor causing difficulties in determining the form of the separation zone is the unsteadiness of the wake. The unsteadiness is especially severe in the flow-past a single cylinder, row, and banks with σ_1, $\sigma_2 \gtrsim 3$ (versions 4 and 6, Table 1). In the average the boundaries of the separation zone are determined at distances 2.5-3.5 of the cylinder radius (althogh in certain cases for small Re the distance is as great as 5 radii). Practically, the configuration of the separation zone is measured completely for version 3, when the separation zone is closed between the two successive cylinders and for version 5 when, due to the strong contraction of the flow, the boundaries of the separation zone close directly in the flow. In the flow past a single row with $\sigma_1 = 2.45$ the interaction of vortex paths is observed. However, there is no explicit evidence of coherence of vibrations of wakes of separate cylinders, which is in agreement with the conclusion of Chen' [7] that a strong correlation of wakes is observed only for $\sigma_1 \lesssim 2$.

We consider in more detail the effect of different factors on the flow-past the cylinder in the bank for version 5 ($\sigma_1 = 2.45$, $\sigma_2 = 1.8$), which is frequently encountered in practice. As has been noted above, it is difficult to determine boundaries of the separation zone visually in the immediate neighborhood of a solid surface. Also, the point of closing of the boundary of the separation zone far from the cylinder is not clearly seem on photographs due to unsteadiness and smooth joining of the paths of the particle-markers. An analysis of the photographs yields negligible scattering of the experimental data, which allows us to conduct a reliable graphical averaging of the paths and to obtain the shape of the separation zone averaged in time. A similar situation takes place also for all other banks of tubes, except for those in the laste row. The analysis of the photographs exhibits also automodeling of the shape of the separation zone with respect to the Reynolds number in the range $Re = 10^3 - 2 \cdot 10^4$, which is confirmed by experiments on other cylinders and banks.

We did not discover an explicit dependence of the shape of the separation zone on the location of the tube in the bank; therefore conclusively established profiles of the separation zone are represented in Fig. 1 as a result of generalization of the data over time, Reynolds number, and the cylinder number. The dots show the continuation of the boundaries of the separation zones behind the halves of the cylinders placed on the wall, since near the solid surface the flow is steadier and the boundaries of the separation zone can be measured at large distances. Except for version 5, when there is a significant contraction of the flow, the profiles of the separation zones are close to each other. A single cylinder has the largest width of the separation zone; the same is true for version 4 with the maximal step σ. In other versions, the contraction of the flow results in the narrowing of the separation zone. In version 3, which is basically close to the unstaggered arrangement, we can clearly see the attachment of a separated flow to the successive cylinder with the angle of attachment $\varphi_п \sim 45°$.

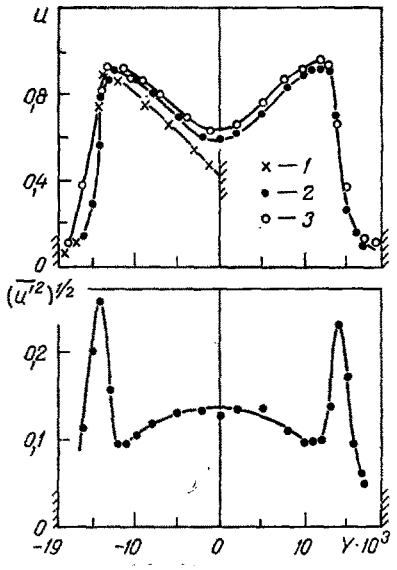

Fig. 2

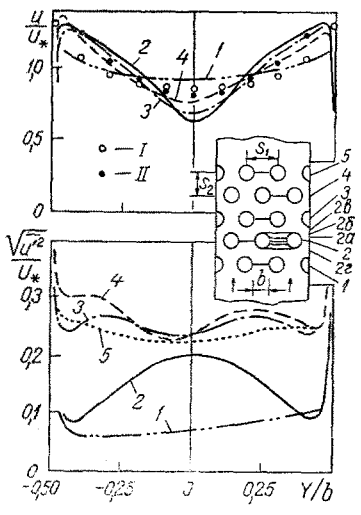

Fig. 3

Fig. 2. Profiles of the averaged velocity u and pulsating velocity $\sqrt{\bar{u}'^2}$ in the cross-section 2b of the 2nd row for Re = $1.6 \cdot 10^4$, X = 8 mm (see the inset in Fig. 3) (version of bank No. 5): 1–3). Number of gaps in the row.

Fig. 3. Profiles of the averaged velocities u/U_* and pulsating velocities $\sqrt{\bar{u}'^2}/U_*$ in the minimal cross-sections of the horizontal rows for Re = $1.6 \cdot 10^4$ (version of the bank No. 5): 1–5, number of cross-sections shown in the inset; I, II, calculations on model [3] for the first and second cross sections, respectively.

The configuration of the separation zones defined in such a way were entered as initial data in the matematical model [3], the results of calculations on which are given in this work.

Velocity Fields. Measurements of velocities were taken in different cross-sections of the staggered bank for versions 3 and 5. An electro-diffusive velocity sensor was introduced in the work site through the side wall. In Fig. 2, typical profiles of the averaged velocity and the level of turbulent pulsations in the cross-section located 8 mm above the axis of the second row (cross-section 2b in Fig. 3) are given. The velocity profile has a form that is characteristic for staggered banks, with the velocity maximum near the boundary of the separation zone (or the cylinder surface) which is due to the contraction and deformation of the flow in the intertube space. We can also distinguish a sharp maximum of the pulsation level near the boundary of the separation zone, which is characteristic for regions with a large velocity gradient. By compring the velocity profiles in different gaps between the cylinders we can draw a conclusion about the symmetry of the flow across the channel. Somewhat lower velocities are observed in the first gap at the wall. The number of gaps is measured from the right wall of the channel.

The evolution of the fields of the averaged and pulsating velocities along the depth of the bank measured in theminimal cross-section of each row is shown in Fig. 3 for the Reynolds number Re = $1.6 \cdot 10^4$. The values of the velocities are refered to the velocity averaged over the given cross-section, which changes from row to row in the range of 5-6% and also differs from the calculated averaged flow rate due to a certain three-dimensionality of the flow. For each gap its own system of coordinates is used with the origin on the axis of the horizontal row in the center of the gap. The X-axis is directed vertically upward, and the Y-axis horizontally to the right. The experimental data in Fig. 3 are given for the second gaps. The designations of the curves correspond to the number of cross-sections shown in the inset. The value of b is the minimal distance between the surfaces of cylinders in the horizontal row and is equal to 32 mm.

As is seen from Fig. 3, a relatively flat velocity profile in the first row acquires the characteristic appearance in the second row. The level of pulsations increases sharply from 7% in the first row to 23% in the third row for Y = 0; however, it practically does not change

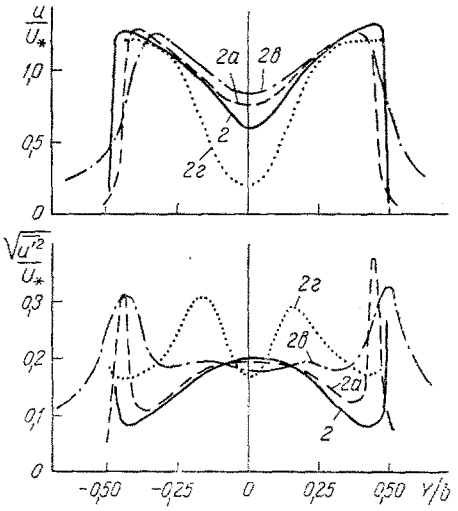

Fig. 4

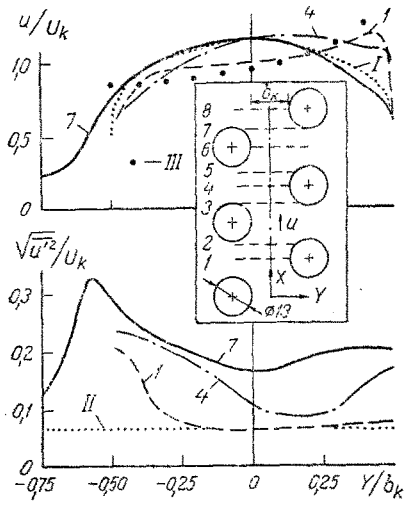

Fig. 5

Fig. 4. The evolution of the profiles of the averaged u/U_* and pulsating $\sqrt{\overline{u'^2}}/U_*$ velocities in the neighborhood of the second row for $Re = 1.6 \cdot 10^4$ (version of bank No. 5): 2-2d, numbers of cross-sections shown in the inset of Fig. 3: 2) X = 0 mm, 2a) 4; 2c) 13; 2d) 11.

Fig. 5. The evolution of profiles of the averaged u/U_* and pulsating $\sqrt{\overline{u'^2}}/U_k$ velocities of $Re_k = 10^4$ (version of bank No. 3); the numbers of curves correspond to the numbers of cross-sections shown in the 1) X = 13 mm; 4) 39; 7) 59; I) turbulent velocity profile in the channel based on formula (I); II) level of pulsations in the incoming flow; III, calculations on the model [3] for the first cross-section.

any more although no complete stabilization is observed either in the averaged velocity or in the pulsation velocity due to the limited number of row.

The Roman numerals I and II designte the results of calculations on the model of an ideal liquid [3] for minimal cross-sections of the first and second rows, respectively. As a whole, the model reflects the main peculiarities of the flow, except for the narrow near-wall region, the boundary layer where the decisive factor is the viscosity. The calculations also give values that are too high in a the near-axis region (immediately after the separation zone) into which the wake from the preceding cylinder extends. The model, however, takes account only of the shape of the separation zone, which is replaced by an equivalent solid body. Similar conclusions also hold for nonminimal cross-sections of the bank.

In Fig. 4, the variation in profiles of the averaged velocity and pulsations along the X-axis in the neighborhood of the second row is shown for $Re = 1.6 \cdot 10^4$. When X increases, the maximum of the velocity shifts toward the X-axis, the minimum of the velocity increases, for Y = 0 and the profile becomes wider. Apparently, the area under the curve, i.e., the flow rate, also changes. However, this is only an apparent unbalance in the flow rate, since the measured velocity profiles cover also the separation zone behind the cylinder, which does not contribute to the general flow rate. In the cross-section 2d the region between two local maxima of pulsations corresponds to the upper part of the separation zone formed behind the cylinder from the first row.

The flow past the bank 4.15 × 1 (version 3), which essentially is a staggered bank (see Fig. 1 and the inset in Fig. 5) is absolutely different. The value of b_k = 14 mm in Fig. 5 is the minimal distance on the Y-axis between the tube surfaces in the adjacent vertical rows, and U_k = 0.7 m/sec is the averaged flow rate corresponding to this gap. The X-coordinate is read from the axis of the first row.

From Fig. 5 it follows that, at first, the unsteady velocity profile (cross-section 1) becomes gradually more symmetric. However, a sufficiently high degree of symmetry is reached only in depth of the bank (cross-section 7). The level of pulsations for Y = 0 increases noticeably from the value 0.07, coinciding with the level of turbulence in the incoming flow (line II), to the value of 0.17 in cross-section 7. As in the preceding version of the bank,

the flow does not stabilize completely. It is noted in the literature that the flow in the unstaggered bank is similar to the case of a flat channel with rough walls. A similar conclusion can be made for the staggered bank 4.15 × 1, since there is a through pasage with width b_k = 14 mm, and a closed separation zone is formed between each pair of successive cylinders (see Fig. 1). Therefore, it is reasonable to use for the analysis of flow the Reynolds number $Re_k = U_k b_k/\nu = 10^4$, and not $Re = U_* d/\nu = 6.2 \cdot 10^3$. Then it is possible to compare experimental data with turbulent profiles in the channel, in the given case, with the 1/7 power law:

$$\frac{U}{U_{max}} = \left(\frac{b_k/2 - |Y|}{b_k/2}\right)^{1/7} \quad (1)$$

(curve I in Fig. 5). As is seen, there is a definite correspondence between the turbulent profile of velocity I for the smooth channel with the profile of velocity 7, although, the complete equivalence between the gap in the unstaggered bank and in the rough channel, apparently, is absent.

Only in case III (i.e., at the bank entrance) can we observe satisfactory agreement between calculations and experiment. In the depth of the bank the discrepancy is more significant. Therefore, model [3] fits best for banks with strongly curved lines of current and can be considered as a basis for creating a method of calculating the aerodynamics of the bank of tubes as applied to the problems of inertial motion of particles and erosion of the surface of tubes when the near-wall effects are unimportant [3].

NOTATION

b, b_k, the distance between the surfaces of cylinders, m; d, cylinder diameter, m; s_1, s_2, transverse and longitudinal steps, m; u, velocity, m/sec; u', velocity pulsation, m/sec; U, U_k, average flow rates, m/sec; U_{max}, maximal velocity, m/sec; X, Y, longitudinal and trasverse coordinates, m; ν, coefficient of kinematic viscosity, m^2/sec; σ_1, σ_2, relative transverse and longitudinal steps φ_a, angle of attachment, rad; $Re = U_* d/\nu$, $Re_k = U_k b_k/\nu$, the Reynolds number.

LITERATURE CITED

1. A. Zhukauskas, R. Ulinskas, and V. Katinas, Hydrodynamics and Vibrations of Flow Past Banks of Tubes [in Russian], Vilnus (1984).
2. I. A. Belov and N. A. Kudryavtsev, Heat Transfer and Resistance of Banks of Tubes [in Russian], Leningrad (1987).
3. S. Yu. Belov, Inzh.-Fiz. Zh, 48, No. 1, 145-146, Dep. at VINITI, No. 5677-84 Dep.
4. V. K. Migai and É. V. Firsova, Heat Exchange and Hydraulic Resistance of Banks of Tubes [in Russian], Leningrad (1986).
5. I. E. Idel'chik, Aerodynamics of Technological Apparatus [in Russian], Moscow (1983).
6. V. E. Nakoryakov et al., Electodiffusion Method of Investigation of the Local Structure of Turbulent Flows [in Russian], Novosibirsk (1986).
7. Chen', Konstruirovanie Tekhnol. Mashinost., 90, No. 1, 137-150 (1968).